LA-UR-04-3385
Approved for public release; distribution is unlimited.

Title: **GADOLINIUM-148 PRODUCTION CROSS SECTION MEASUREMENTS FOR 600- AND 800-MEV PROTONS**

Author(s): Karen Kelley[1,2], Matt Devlin[1], Eric Pitcher[1], Stepan Mashnik[1], Nolan Hertel[2]
[1]Los Alamos National Laboratory, Los Alamos, New Mexico 87544
[2]Georgia Institute of Technology, Atlanta, Georgia 30332-0425

Submitted to: Proc. of the Seventh Meeting on Shielding Aspects of Accelerators, Targets and Irradiation Facilities (SATIF-7), Instituto Technologico e Nuclear (ITN) Sacavem (Lisbon) Portugal, May 17-18, 2004

http://lib-www.lanl.gov/cgi-bin/getfile?00783499.pdf

GADOLINIUM-148 PRODUCTION CROSS SECTION MEASUREMENTS FOR 600- AND 800-MEV PROTONS

Karen Kelley[1,2], Matt Devlin[1], Eric Pitcher[1], Stepan Mashnik[1], Nolan Hertel[2]
[1]Los Alamos National Laboratory, Los Alamos, New Mexico 87544
[2]Georgia Institute of Technology, Atlanta, Georgia 30332-0425

Abstract

In a series of experiments at LANSCE's WNR facility, ^{148}Gd production was measured for 600- and 800-MeV protons on tungsten, tantalum, and gold. These experiments used 3 μm thin W, Ta, and Au foils and 10 μm thin Al activation foils. Gadolinium spallation yields were determined from these foils using alpha spectroscopy and compared with the LANL codes CEM2k+GEM2 and MCNPX.

Introduction

When heavy metal targets, such as tungsten, are bombarded with protons greater than a few hundred MeV many different nuclides are produced. These nuclides are both stable and radioactive and are created by spallation, proton activation, or secondary reactions with neutrons and other nuclear particles made in the target. These products are distributed somewhat heterogeneously throughout a thick target because of the energy dependence of the cross sections and energy loss of the proton beam within the target. From this standpoint, it is difficult to measure nuclide production cross sections for a given energy proton in a thick target.

At the Los Alamos Neutron Science Center (LANSCE) accelerator complex, protons are accelerated to 800 MeV and directed to two tungsten targets, Target 4 at the Weapons Neutron Research (WNR) facility and 1L target at the Manuel Lujan Jr. Neutron Scattering Center. DOE requires hazard classification analyses to be performed on these targets and places limits on radionuclide inventories in the target as a means of determining the "nuclear facility" category level [1]. Presently, WNR's Target 4 is a non-nuclear facility while the Lujan 1L target is classified as a Category 3 nuclear facility. Gadolinium-148 is a radionuclide created from the spallation of tungsten and other heavy elements. Allowable isotopic inventories are particularly low for this isotope because it is an alpha-particle emitter with a 75-year half-life. The activity level of ^{148}Gd is generally low, but it encompasses almost two-thirds of the total inhalation dose burden in an accident scenario for the two tungsten targets at LANSCE based on present yield estimates [2,3]. From a hazard classification standpoint, this severely limits the irradiation lifetime of these tungsten targets.

As 800-MeV protons pass through the tungsten targets at WNR and the Lujan Center, the proton energy is degraded to 600 MeV upon exiting the target. Since the facility classification is partly driven by the inventory of ^{148}Gd, a better estimate of the true production rate in tungsten targets is needed.

From a basic nuclear physics standpoint, the ideal strategy would be to measure the ^{148}Gd production cross sections for each tungsten isotope. However, obtaining isotopically pure tungsten foils was not feasible. An alternative was to perform measurements with a mono-isotopic element with an atomic number close to that of tungsten (Z=74). Tantalum (Z=73), which is 99.988% ^{181}Ta, provides a good alternative for testing the physics models used to estimate spallation products at these energies. Furthermore, tantalum is used as target cladding materials at the KENS (Japan) and ISIS (United Kingdom) spallation neutron source facilities. These facilities operate at 500 MeV and 800 MeV, respectively. By measuring production from Ta, nuclear physics models can be used in conjuction with production cross section measurements from elemental W, to gain a better understanding of production rates for individual W isotopes, and help evaluate dose burdens at other spallation neutron source facilities. Another mono-isotopic element of interest to the spallation target community is gold (Z=79), which is next to mercury (Z=80) in the periodic table. Mercury is the planned target material for the Spallation Neutron Source being built at Oak Ridge National Laboratory.

The ^{148}Gd inventory in a thick target is difficult to deduce because ^{148}Gd decays only by alpha-particle emission with no associated gamma-ray emission. To date, only one measurement of the number of ^{148}Gd atoms produced in tungsten has been made. A radiochemistry analysis, done as part of the Accelerator Production of Tritium Project decay heat experiment, measured

the number of ^{148}Gd atoms in the center of three tungsten foils irradiated with 800-MeV protons [4,5]. Assuming that the isotope is only produced within the beam spot, a cumulative cross section of 16.40±0.41 mb can be inferred from this measurement. Cumulative yields include production from the decay of radioactive parents. A current theoretical estimate by Mashnik *et al.*'s CEM2k+GEM2 code [6] for cumulative production for tungsten is 41.4±0.4 mb at 800 MeV and 21.6±0.3 mb at 600 MeV. The default physics models of MCNPX (Bertini internuclear cascade + MPM preequilibrium + Dresner evaporation with GCCI level density + RAL fission, hereafter referred to as "Bertini") [7] yields 20.9±1.6 mb at 800 MeV and 10.9±0.2 at 600 MeV for cumulative production from elemental W. Because the accuracy of predicting the cumulative ^{148}Gd production cross section by the Bertini model is unknown, the procedure approved by DOE regulators for calculating the ^{148}Gd inventory in the targets requires the value predicted to be multiplied by a factor of two in order to account for this uncertainty. This uncertainty factor further limits the lifetime of the target. A comparison of independent and cumulative production yields from CEM2k+GEM2, Bertini, and the APT measurement can be found in Figure 1. This figure shows that the independent ^{148}Gd production contribution is only 5 to 15% of the cumulative ^{148}Gd production for CEM2k+GEM2, whereas Bertini indicates that this contribution is 30 to 45%. The dominant factor between the cumulative ^{148}Gd production cross sections is the difference in ^{152}Er production (Table 1). Figure 2 shows the independent production cross sections as a function of product mass and Z for Z=64 to 72. These rare earth curves indicate that CEM2k+GEM2 typically predicts a higher cross section for the lower masses than Bertini for a given Z, whereas Bertini predicts a higher cross section for the higher masses for a given Z. These figures and tables demonstrate how different these two intranuclear cascade models are in calculating production yields for the rare earth metals.

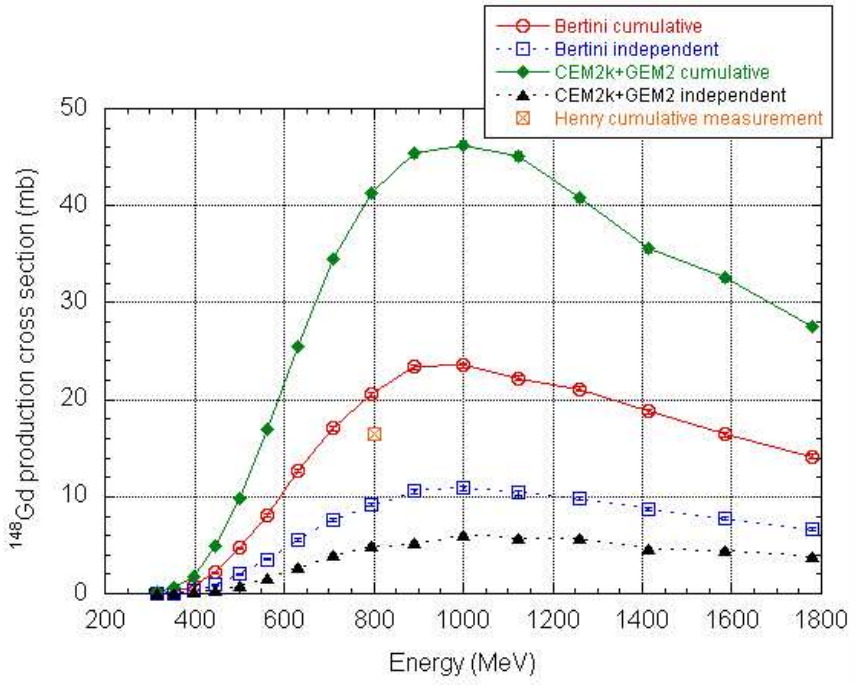

Figure 1: Calculated ^{148}Gd production cross sections for W(p,x)^{148}Gd by CEM2k+GEM2, Bertini in MCNPX, and an inferred measurement from APT.

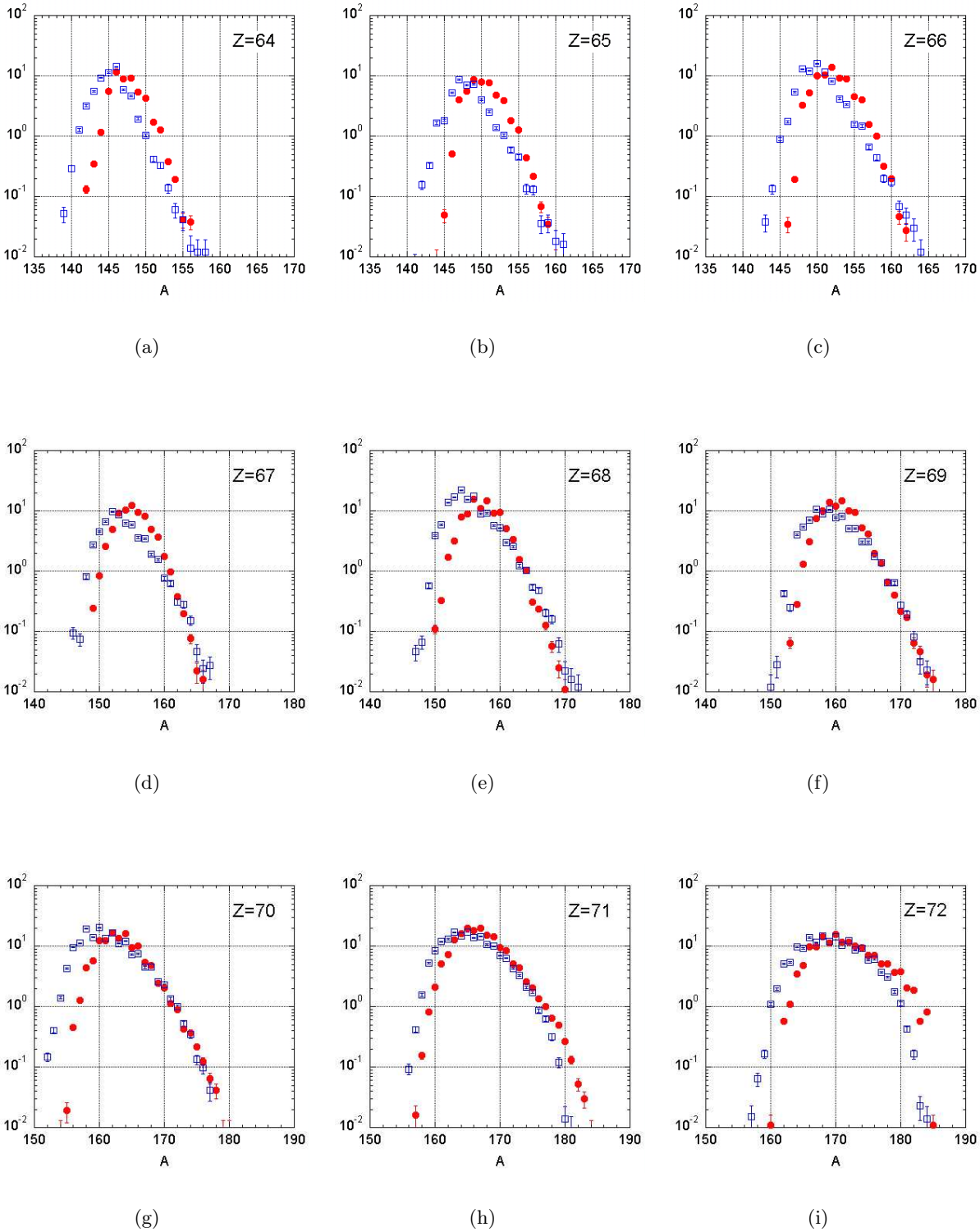

(a) (b) (c)

(d) (e) (f)

(g) (h) (i)

Figure 2: Independent radionuclide production curves from 800 MeV protons incident on tungsten for Z=64 to 72. Open blue squares represent CEM2k+GEM2 and red-filled circles represent Bertini.

Table 1: Comparison of independent radionuclide production cross sections used in calculating the cumulative ^{148}Gd production cross sections from 800-MeV protons incident on tungsten for Bertini and CEM2k.

	% contribution to cumulative	Independent cross section (mb)		Bertini/CEM2k ratio
		Bertini	CEM2k	
^{148}Gd	100	9.26±1.58	4.65±0.14	1.99
^{148}Tb	100	5.59±0.13	6.98±0.17	0.80
^{148}Dy	100	3.28±0.10	12.9±0.2	0.25
^{148}Ho	100	0.003±0.003	0.812±0.058	0.003
^{152}Dy	0.1	13.9±0.19	8.17±0.18	1.71
^{152}Ho	23.0	4.87±0.12	9.56±0.20	0.51
^{152}Er	91.2	1.72±0.07	13.7±0.2	0.13
^{152}Tm	91.2	0.003±0.003	0.428±0.042	0.006
^{156}Tm	0.007	3.08±0.09	7.07±0.17	0.44
^{156}Yb	9.13	0.455±0.035	9.52±0.20	0.048
^{156}Lu	86.6	0.000±0.000	0.093±0.019	0.00
^{160}Hf	0.064	0.011±0.005	1.11±0.07	0.010

Methods

In order to accurately assess the production of ^{148}Gd in a thick target within the range of 600 to 800 MeV, a series of thin or thick target experiments within the energy range of interest must be performed. There are several methods by which ^{148}Gd production can be determined. One method is a thick target experiment, where a cylindrical target similar to the ones at LANSCE is irradiated. The target would be cut into thin slices to determine production within small proton energy intervals since the initial proton energy is degraded as it passes through the target. The irradiated target would then be destructively assayed to determine quantities of isotopes produced. By measuring the production rate of ^{148}Gd as a function of depth in a target, the amount of this isotope created as a function of proton energy can be deduced. The primary drawback to this method is contamination by high-energy secondary protons.

Another method is to irradiate thin foils at specific proton energies to obtain production cross sections. Nuclear reaction models can then normalize the production cross section from threshold to 800 MeV for an array of heavy metals (tungsten, tantalum, and gold). Thin foil experiments allow foils of different materials to be irradiated at the same time. Since the proton energy loss through each foil is negligible, all foils are essentially exposed to a single proton energy. Not only do the foils need to be thin enough to have negligible energy loss during irradiation, they also need to be thin enough for ^{148}Gd decay alphas to later escape and be detected. The foil thickness without permanent mylar support backing was 3 μm for tungsten, tantalum, and gold and 10 μm for aluminum, based on ^{148}Gd's α range. It was decided to use the thin foil method for measuring the ^{148}Gd production cross section because it could help evaluate dose burdens at spallation neutron source facilities and aid the nuclear physics models community.

A proposed foil stack to be irradiated would consist of one aluminum foil, three tungsten,

tantalum, or gold foils, followed by three aluminum foils. Aluminum foils are used to determine the proton flux using the well-known ^{27}Al(p,x)^{22}Na reaction. Eight measurements exist for 800-MeV protons, and two measurements exist for 600-MeV protons [8-16]. Our conclusion from a survey of available experimental data is that Morgan *et al.*'s recent measurement at 800 MeV [9] and Tobailem *et al.*'s measurement in 1981 at 600 MeV [8] are most reliable. These cross section values, 14.3±0.4 mb and 16.0±1.1 mb, at 800 and 600 MeV respectively, were used in our analysis. Stacks of three foils are used to investigate any possible loss of ^{148}Gd and ^{22}Na recoils in the material of interest. When determining the proton flux and production cross section, only the middle foils are counted where recoil from the first foil balances the loss by recoil to the third foil.

Another method is to irradiate only one foil, sandwiched between two aluminum foils. In this case, the sum of ^{148}Gd counted from the heavy metal foil and the two aluminum foils would be used to determine the production cross section. This approach is viable because ^{148}Gd is not produced by spallation reactions in Al.

The proton flux for a known reaction cross section σ of ^{27}Al(p,x)^{22}Na can be found by

$$\phi_p = \frac{1}{N_{Al}\sigma_{Na}} \frac{C_{Na}\ \lambda_{Na}}{\epsilon_{Na}\,(1 - e^{-\lambda_{Na}t_i})\,(e^{-\lambda_{Na}t_1} - e^{-\lambda_{Na}t_2})} \tag{1}$$

where N is the number of atoms, λ is the decay constant, C is the integral number of counts, ϵ is the detection system efficiency, $t_i > 0$ is the total irradiation time, and $t_2 - t_1$ is the detection counting time where $t_1 > t_i$. One can then use the proton flux to determine a production cross section for W(p,x)^{148}Gd.

$$\sigma_{Gd148} = \frac{1}{N_W\phi_p} \frac{C_{Gd}\ \lambda_{Gd}}{\epsilon_{Gd}\,(1 - e^{-\lambda_{Gd}t_i})\,(e^{-\lambda_{Gd}t_1} - e^{-\lambda_{Gd}t_2})} \tag{2}$$

Irradiations

A series of foil irradiations at 600 and 800 MeV have taken place in the Blue Room at WNR. Anticipated beam spot sizes were 1 cm in diameter, so each foil had to be sufficiently large enough, 5 cm x 5 cm, to subtend all of the proton beam. Individual foils were sandwiched between aluminum frames for ease of handling. Framed foils were then stacked together and mounted on a larger frame that centered the foils inside the vacuum chamber. Up to four foil stacks could be placed in the vacuum chamber in the Blue Room, upstream of the last steering magnet for Target 4. A phosphor was also placed in the vacuum box to aid in positioning and shaping the beam spot on the foils.

The irradiations took place in two modes, sole use and parasitic. Behind the steering magnet is Target 4 at WNR, where neutrons are produced and scattered to different beamlines for experiments. When in sole use, Target 4 was used as a beam stop, not for production of neutrons. In parasitic mode, the proton beam passed through the foils and then on to Target 4 for neutron production. The energy loss through the foils was negligible (<0.11 MeV) so all the foils saw essentially the same energy, with no proton energy loss to Target 4. It was determined

that as much as 30 mg/cm^2 could be placed in the beam without significantly degrading the neutron production from Target 4.

After the irradiations, the aluminum foils were counted using a HPGe detector system to detect the 1274-keV emission line of ^{22}Na (2.6 year half-life) to determine the integrated proton flux. These proton flux measurements compared well (within 10%) of the current monitors (3% uncertainty) upstream of the Blue Room (Table 2).

Table 2: Irradiations performed in the Blue Room at WNR during the 2002-2003 run cycle. Each irradiation measured the proton flux with Al foils for ^{22}Na activation and current monitors upstream of Blue Room

Metal Foils	Singles or Stacked Foils	Mode of operation	E_p (MeV)	Integrated ϕ_p (p/s) ^{22}Na Activation	Integrated ϕ_p (p/s) Current Monitor	Ratio of ^{22}Na to Monitor
W, Ta, Au	stacks of 3	sole use	600	1.76×10^{13}	1.63×10^{13}	1.08±0.09
Ta	stacks of 3	parasitic	800	1.42×10^{13}	1.32×10^{13}	1.08±0.05
Au	stacks of 3	parasitic	800	2.38×10^{13}	2.32×10^{13}	1.03±0.05
W	stacks of 3	parasitic	800	2.41×10^{13}	2.48×10^{13}	0.972±0.049
W, Ta, Au	singles	sole use	800	1.83×10^{13}	1.72×10^{13}	1.06±0.05

Results

Each foil was counted by a Si charged-particle semiconductor detector in vacuum to measure ^{148}Gd production. Gadolinium-148 alpha emission occurs at 3.183 MeV and the α-particle loses up to 2.5 MeV of its energy passing through as much as 3 μm of foil thickness before depositing its remaining energy in the detector [18]. So a broad, level, α peak was expected ranging from about 1.0 to 3.2 MeV, assuming that ^{148}Gd is evenly created throughout the thickness of the foil.

A wide energy range of β and γ particles from various radionuclides were also emitted from the foils and deposited only a portion of their energy in the detector. This complicated the α counting since the lower energy portion of the α peak was superimposed on this $\beta + \gamma$ background. One way to solve this problem was to place a sufficiently thick aluminum foil in front of the irradiated foil to block all α's from reaching the detector so that only $\beta+\gamma$ particles were detected. The $\beta + \gamma$ spectrum could then be subtracted from the combined $\alpha + \beta + \gamma$ spectrum to produce a clean α peak. Representative charged-particle spectra of tungsten and tantalum foils irradiated at 800 MeV are shown in Figures 3,4. The separation between the ^{148}Gd α peak and the $\beta+\gamma$ spectrum is distinct for tantalum, but not for tungsten and gold. In the case of tungsten and gold, two separate counts were used to produce the α spectra–one bare foil to measure the $\alpha + \beta + \gamma$ spectrum and one with a thin Al α absorber in front to measure the $\beta + \gamma$ spectrum. The number of counts in this $\beta + \gamma$ spectrum could then be subtracted from the combined $\alpha + \beta + \gamma$ spectrum to produce the α spectrum.

Table 3 summarizes the cumulative ^{148}Gd production measurements and previous measurements, CEM2k+GEM2, and Bertini for W, Ta, and Au. The production cross sections measured at 600 MeV were 15.2±4.0, 8.31±0.92, and 0.591±0.155 for Ta, W, and Au, respectively. The

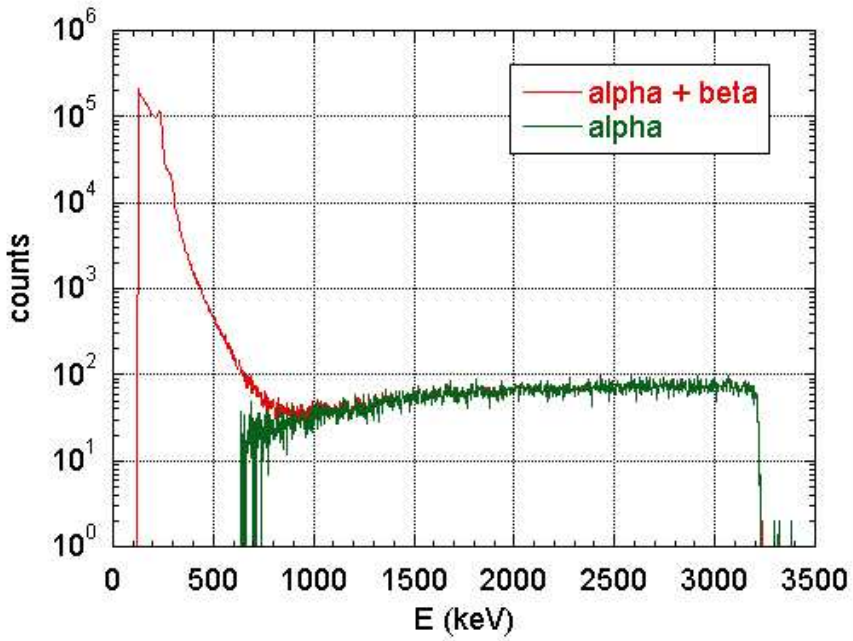

Figure 3: Charged particle spectrum of W7 from the 800-MeV stacked foil irradiation. Counting time was 3 days.

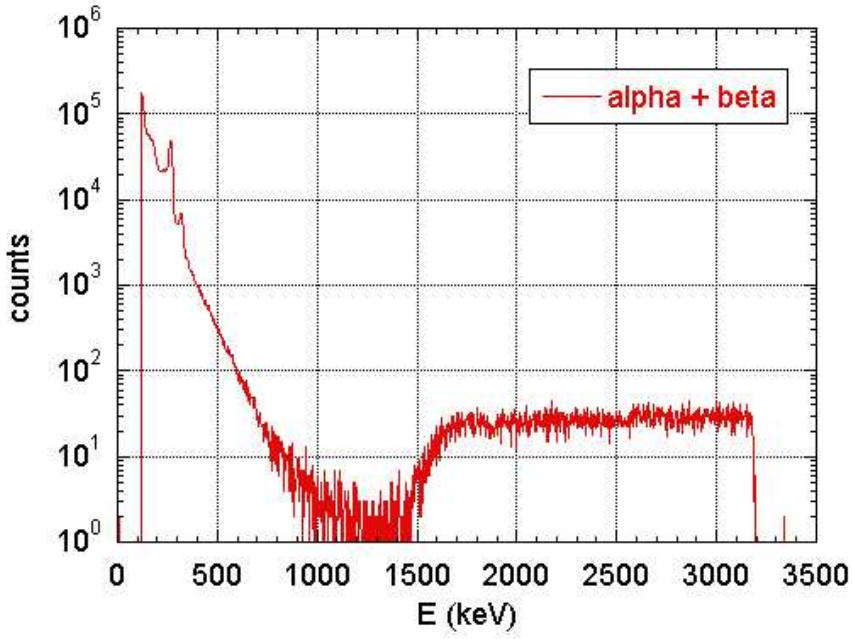

Figure 4: Charged particle spectrum of Ta5 from the 800-MeV stacked foil irradiation. Counting time was 2 days.

average production cross sections measured at 800 MeV were 28.6±3.5, 19.4±1.8, and 3.69±0.50 for Ta, W, and Au, respectively. The average measurement for W at 800 MeV was 18% higher than the previous measurement by Henry and the average for Au at 800 MeV was 2% less than the previous measurement by Rejmund, et al. Theoretically, the Bertini model better predicted the ^{148}Gd production than CEM2k+GEM2. Results using the Bertini model ranged from 2-25% of the Ta and W measurements and 35-50% higher than the Au measurements. The CEM2k+GEM2 predictions were a factor of two to three higher than the measurements. The comparisons for both Bertini and CEM2k+GEM2 were best for Ta and worst for Au. This was possibly due in part to the fact that Ta is closer in nucleon number to Gd, compared to W and Au, and therefore it is easier to predict ^{148}Gd from the spallation of Ta.

Table 3: Cumulative ^{148}Gd production cross section measurements and comparisons to theoretical predictions and previous measurements

			^{148}Gd cumulative production cross section (mb)			
	Energy	Foil	Current	Previous	Theoretical	
Target	(MeV)	Setup	Measurement	Measurement	CEM2k+GEM2	Bertini
Ta	600	stacked	15.2±4.0		29.4±0.2	15.5±0.2
	800	stacked	29.7±7.6		45.6±0.3	24.4±0.3
		single	27.6±1.7			
		single	28.6±7.3			
W	600	stacked	8.31±0.92		21.6±0.3	10.9±0.2
	800	stacked	19.5±1.2	16.4±0.8[a]	41.4±0.4	20.9±1.6
		single	18.0±1.1			
		single	20.7±5.3			
Au	600	stacked	0.591±0.155		1.41±0.04	0.929±0.049
	800	stacked	3.86±0.98	3.74±0.19[b]	12.9±0.1	7.23±0.14
		single	3.52±0.22			

[a] [5] Henry *et al.* APT Internal Report, LLNL 1999.
[b] [17] Rejmund *et al. Nucl Phy A*683 2001 540-565.

Conclusions

Measuring the ^{148}Gd production cross section from protons on tungsten, tantalum, and gold is of great benefit to the spallation neutron source community. A better estimate of the ^{148}Gd yield, and as a result, a better estimate of the dose burden might extend the irradiation lifetime of spallation targets.

A series of thin foil irradiations have been completed with 600- and 800-MeV protons on tungsten, tantalum, gold, and aluminum. The ^{148}Gd production cross section measurements for tungsten and gold agree well with previous measurements. Theoretical predictions using the Bertini model agree better than CEM2k+GEM2, and all predictions are within a factor of two to three.

REFERENCES

[1] DOE Technical Standard DOE-STD-1027-92, 1992.

[2] Jeffrey S. Bull *et al.*, LANL Report 53-BIO-004, Rev.2, 2000.

[3] Jeffrey S. Bull, LANL Internal Report CN-LANSCEFM-00-001, 2000.

[4] D. L. Quintana *et al.*, *ANS Proc 4th Intl Top Mtg Nucl App Acc Tech*, 2000 405-414.

[5] E. A. Henry and K. J. Moody, APT Internal Report, LLNL 1999.

[6] S. G. Mashnik *et al.*, LANL Reports LA-UR-02-0608, 2002; LA-UR-03-2261, 2003.

[7] L. S. Waters *et al.*, LANL Report LA-CP-02-408, 2002.

[8] J. Tobailem, Report CEA-N-1466(5), 1981.

[9] G. L. Morgan *et al.*, *Nucl Inst Meth B*211, 2003 297-304.

[10] R. Michel *et al.*, *Nucl Inst Methods B*103, 1995 183-222.

[11] T. N. Taddeucci *et al.*, *Phys Rev C*55, 1997 1551-1554.

[12] H. R. Heydegger *et al.*, *Phys Rev C*14(4), 1976 1506-1514.

[13] G. I. Krupnyi, D. V. Snitko, A. A. Yanovich, *Atomic Energy* 89(5), 2 939-941.

[14] H. Vonach *et al.*, *Phys Rev C*55(5), 1997 2458-2467.

[15] W. R. Webber, J. C. Kish, D. A. Schrier, *Phys Rev C*41(2), 1990 547-565.

[16] G. M. Raisbeck and F. Yiou, *Phys Rev C*9(4), 1974 1385-1395.

[17] F. Rejmund *et al.*, *Nucl Phys A*683, 2001 540-565.

[18] J. F. Ziegler and J. P. Biersack, SRIM version 2000.40, 2000. SRIM website http://www.srim.org